

Fish from the sky: Airborne eDNA tracks aquatic life

Yin Cheong Aden Ip^{1*}

Gledis Guri^{1*}

Elizabeth Andruszkiewicz Allan¹

Ryan P. Kelly¹

2025-06-03

School of Marine and Environmental Affairs, University of Washington, Seattle,
Washington, USA

* shared first authorship

corresponding author adenip@uw.edu

Teaser

Aquatic life leaves traces in the air, opening a new frontier in passive biodiversity monitoring.

Abstract

Water and air are generally treated as separate reservoirs of environmental DNA (eDNA) derived from the species resident in those respective environments. However, it is likely that eDNA routinely crosses the air-water boundary in both directions as a result of deposition, evaporation, or other processes. Here, we systematically tested methods of sampling eDNA at the air-water interface, showing for the first time that aquatic life can be reliably detected from passive air samples collected nearby. We deployed four simple air samplers — three different kinds of filters and one open tray of deionized water — alongside paired water samples and visual counts over a six-week peak run of Coho salmon (*Oncorhynchus kisutch*) at a local spawning stream. We then quantified eDNA concentrations in both air and water (air: copies/day/cm²; water: copies/L) using quantitative PCR, to estimate (1) the concentration of target eDNA in air vs. water, and (2) the capture performance of each filter type. Despite an approximate 25,000-times dilution versus water, passive air collectors captured quantitative airborne eDNA signals that closely paralleled salmon counts, although recovery varied with sampler design and orientation. We show the air-water interface is a quantifiable source of aquatic genetic information using simple, passive samplers that do not require electricity, making them appealing for biomonitoring in remote or resource-limited settings. This work points the way to using airborne

28 eDNA as a robust pathway for biological information critical to conservation, resource
29 management, and public-health protection.

30 **Keywords:** environmental DNA, Air eDNA, Passive Air Filtration, Aquatic Biomonitoring,
31 Aerosolization, Evaporation, Non-invasive Sampling, Quantitative eDNA Analysis, Salmon,
32 Environmental Genomics

33 Introduction

34 Monitoring aquatic life is fundamental to understanding ecosystem health, guiding conservation
35 efforts, and managing valuable natural resources (1, 2). Over the past decade, environmental
36 DNA (eDNA) has upended our paradigm for biodiversity assessment by detecting and
37 quantifying organisms through the genetic material they shed into their surroundings. Water-
38 based eDNA surveys have proven particularly effective for monitoring endangered species ((3)),
39 early detection of invasive species incursions ((4)), characterizing community composition ((5)),
40 and even providing quantitative assessments for complementing traditional surveys ((6–8)).

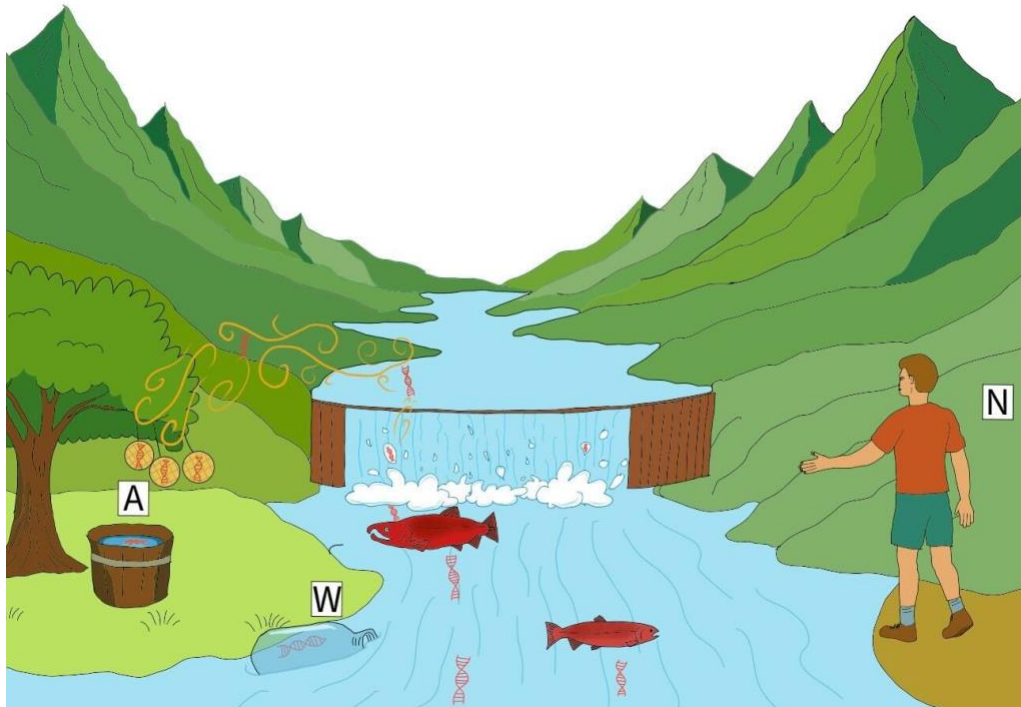
41 Meanwhile, airborne eDNA research has emerged as a promising frontier, though to date it has
42 focused almost exclusively on terrestrial organisms. Both active and passive air filtration
43 methods have been shown to recover DNA from mammals, birds, insects, and plants under field
44 and enclosed conditions ((9–15)). Intriguingly, these same air-sampling techniques sometimes
45 detect strictly aquatic taxa. Yet in almost every case, these signals were never the focus of the
46 study and are often treated as suspected contamination or attributed to zoo feed or piscivores
47 fecal bioaerosols (15–18), rather than recognized as a genuine ecological signal (19).

48 Aquatic species signals detected in airborne eDNA surveys are often discarded (17, 18, 20, 21).
49 Yet, these overlooked detections hint at a genuinely unexplored, rich, untapped source of data for
50 a complementary biodiversity monitoring approach. Environmental systems are inherently
51 interconnected (22), and basic physics points to why aquatic DNA should appear in air (23, 24).
52 Natural physical processes at the air-water interface, such as evaporation, bubble-burst
53 aerosolization from ripples and splashes, and leaping fish, churning substrates, create splash-
54 driven aerosols; all of these provide plausible mechanisms for transferring eDNA into the
55 atmosphere (25–28). These potential mechanisms would suggest that air could act as a diluted,
56 but still informative, extension of the aquatic environment, representing biological signals that
57 are real, quantifiable, and ecologically meaningful.

58 To test this hypothesis, we conducted the first targeted investigation of cross-medium water-to-
59 air eDNA transfer, specifically examining whether genetic material from aquatic organisms can
60 be detected in air samples collected above water surfaces. Leveraging the behavior of Coho
61 salmon (*Oncorhynchus kisutch*) during their spawning season (26), we collected and measured
62 eDNA concentrations in paired water and passive air samples over a six-week peak migration
63 period, with visual fish counts from hatchery staff. To evaluate the mechanisms of airborne DNA
64 capture and settlement, we deployed four passive air collection methods: vertically orientated
65 gelatin air filters (commonly used in low-flow air filtration systems), polytetrafluoroethylene
66 filters (PTFE; standard in high-flow air applications), and mixed cellulose ester filters (MCE;
67 traditionally employed for water filtration), as well as an open, horizontal tray of deionized water
68 exposed to ambient conditions (17). These were chosen for their distinct physical properties,

69 contrasting orientations, and different particle capture efficiencies targeting different aerosol
70 types. By comparing detection sensitivity, temporal patterns, and quantitative performance of
71 these four collectors against water eDNA concentrations and visual counts, we show that—even
72 at roughly 25,000-times dilution—airborne eDNA can reliably track real-world aquatic
73 population dynamics.

74 Our findings provide the first evidence that aquatic genetic material can indeed transfer from
75 water to air under natural conditions, and extends further with quantitative demonstrations that
76 reflect actual population dynamics with just passive air samplers. Far from weighing air against
77 water sampling, this cross-medium detection and quantification represents not merely a technical
78 advancement, but a conceptual leap in ecological monitoring: the previously ignored air–water
79 interface now emerges as a measurable reservoir of aquatic genetic information. While this study
80 centers on salmon, its implications extend broadly, proving that aquatic eDNA in the air is
81 quantifiable and potentially species rich. This advancement re-imagines ecological monitoring as
82 one that bridges water and air to build more resilient, comprehensive surveillance networks in a
83 rapidly changing world. Such integrated approach can become particularly valuable during
84 extreme environmental conditions—when droughts parch rivers, floods render wading unsafe, or
85 public-health concerns close off contaminated waters (29–31)—indicating that airborne eDNA
86 can offer a complementary pathway for capturing aquatic genetic signals.



87
88 *Figure 1: Conceptual illustration of cross-medium eDNA sampling above a salmon-spawning stream.*
89 *Natural processes, including evaporation, bubble-burst aerosolization at riffles and splashes, and the*
90 *vigorous movement of spawning Coho salmon, launch trace amounts of DNA from the river surface into*
91 *the atmosphere. Passive airborne samplers, shown here as three vertically hung filters and an open tray*

92 of deionized water (*A*), intercept settling airborne eDNA, while paired water-grab sampling (*W*) and
93 visual counts by hatchery staff (*N*) provide concurrent reference measurements.

94 Methods

95 Field Sampling

96 We conducted this study in Issaquah Creek, a salmon spawning stream, outside of the Issaquah
97 Salmon Hatchery (47.529501° N, 122.039133° W) from 26 August 2024 to 18 November 2024,
98 with nine sampling events. We chose nine field trips that spanned the entire coho salmon
99 (*Oncorhynchus kisutch*) run, from the first arrivals in early fall of August, through peak
100 abundance around 17 October 2024 and into the tail end of the migration in November. This
101 schedule ensured that our eDNA sampling captured both the lowest and highest levels of fish
102 activity. Within the same sampling period, visual fish counts were performed by the hatchery
103 staff, and salmon escapement data were obtained from the Washington Department of Fish and
104 Wildlife
105 escapement reports
106 (<https://wdfw.wa.gov/fishing/management/hatcheries/escapement#2024-weekly>). Throughout
107 our nine sampling events, weather conditions ranged from clear, calm days to periods of rainfall;
108 detailed records of air temperature, wind speed, relative humidity, and precipitation are provided
in Supplementary Material 1.

109 Sampling for eDNA was conducted in 24-hour blocks with deployment and recovery around 9
110 a.m. (river water was collected only on the first day/timepoint). Four passive collection methods
111 were evaluated: three filter types—gelatin (Sartorius, 47 mm diameter), PTFE (Whatman, 47
112 mm diameter), and MCE (Stereulitech, 5.0 µm pore size, 45mm diameter)—and an open container
113 of deionized water. The rationale for selecting these materials is as follows: gelatin filters are
114 effective at capturing airborne particles and are particularly suited for applications where
115 maintaining viability (e.g., for subsequent bacterial culturing; (32)) is desired; PTFE filters are
116 noted for their high durability and are widely used in active air sampling experiments (33);
117 whereas MCE filters, typically employed for water filtration, were included to assess their
118 performance in an airborne context (6). All three passive filters were deployed via custom 3D-
119 printed “honeycomb” puck filter holders, based on open-source Thingiverse designs (IDs
120 4306478 and 979318; Zachary Gold, pers. comms.), and were suspended from a hatchery railing
121 approximately 3 m above the river water level (Figure 1), with their collection surfaces oriented
122 horizontally. All three passive filters were deployed via 3D-printed “honeycomb” puck holders,
123 based on open-source Thingiverse designs (IDs 4306478 and 979318)¹ and generously shared by
124 Mautz et al. (2025).

125 This configuration minimizes splash contamination and captures airborne DNA particles driven
126 by gravitational settling. The positioning relative to flowing water demonstrates how these
127 passive collectors operate at a vantage point above the stream, facilitating non-invasive DNA
128 capture in real-world field conditions. Two biological replicates were deployed for both gelatin
129 and PTFE, while only one replicate was used for MCE. After the overnight deployment, filters
130 were carefully recovered using sterile, disposable forceps and immediately immersed in 1.5 mL
131 of DNA/RNA Shield.

¹ <https://www.thingiverse.com/thing:4306478>; <https://www.thingiverse.com/thing:979318>

132 The fourth passive collection method was an open container (25 cm width, 30 cm length, 10 cm
133 depth) filled with 2 L of deionized water (17) also positioned about 3 m above the river and
134 about 30 cm above the suspended passive filters. The open container was also deployed for about
135 24 hours at the same times as the passive filters. The container had an open surface (i.e., oriented
136 horizontally) to capture airborne particles settling by gravity. The surface area of the container
137 was approximately 750 cm², in contrast to the roughly 16 cm² surface area offered by the 47-
138 mm circular filter disks. Only one replicate was used for the open water container method. Note
139 that although 2 L of deionized water was placed in the container, heavy rainfall during overnight
140 deployments sometimes increased the water level. Any debris (e.g., bugs, leaves) was removed
141 from the container before on-site filtration using the same system as for river water samples (see
142 below for details).

143 Concurrent with airborne sampling, water samples were collected by hand from the river directly
144 adjacent to the coho salmon aggregation school, just downstream of the fish ladder entrance. The
145 ladder is operated continuously by hatchery staff throughout the salmon run, ensuring fish
146 passage and visual counts. A total of 3 L of water was filtered on site using a Smith-Root Citizen
147 Science Sampler equipped with 5.0 µm mixed cellulose ester (MCE) filters (6). Three 1 L
148 replicates were processed and immediately preserved in 1.5 mL of DNA/RNA Shield (Zymo
149 Research) using clean disposable plastic forceps. Field-negative filtration blanks (1 L of Milli-Q
150 water each) were also processed using the same system. All equipment was decontaminated with
151 10% bleach, thoroughly rinsed with deionized water, and handled with gloves to minimize
152 contamination. All filters (passive air, passive open container, water) were stored at -20°C until
153 processing, typically within one week.

154 **Wet-Laboratory Procedures**

155 DNA extraction from both river water samples and airborne filter samples was performed using
156 the Qiagen Blood and Tissue Kit according to the manufacturer's protocols. During extraction, it
157 was noted that the gelatin filters dissolved completely in the DNA/RNA Shield. Samples were
158 vortexed for 1 minute, and 500 µL of the shield was used for DNA extraction.

159 qPCR assays targeted a 114-bp fragment of the cytochrome b gene of coho salmon, using
160 primers derived from (34)— COCytb_980-1093 Forward:
161 CCTTGGTGGCGGATATACTTATCTTA and COCytb_980-1093 Reverse:
162 GAACTAGGAAGATGGCGAAGTAGATC. SYBR Green chemistry was employed using
163 SYBR Select Master Mix (Fisher Scientific) on an Applied Biosystems QuantStudio 5 real-time
164 PCR system with a 384-well block. Each 10 µL reaction consisted of 5 µL of SYBR Select
165 Master Mix, 0.4µL of 10 mM forward primer, 0.4 µL of 10 mM reverse primer, 2.2 µL of
166 molecular grade water, and 2 µL of DNA template. Melt curve analysis was performed to
167 confirm the amplification of the target fragment, with an accepted melting temperature of 81°C ±
168 1°C.

169 Standard curves were constructed using a coho tissue DNA extract quantified with a Qubit
170 fluorometer. The stock solution was diluted to 1.0 ng/µL and designated as 10⁶ copies/µL. Serial
171 dilutions were then prepared, with 10⁵, 10⁴, and 10³ copies/µL run in triplicate, 10² copies/µL in
172 quadruplicate, and 10¹/µL copies in triplicate.

173 **Joint statistical model**

174 **Visual observation model**

175 In summary, we synthesize three methods of observations (visual counting of fish, water eDNA
176 measurements, and air eDNA measurements) which derive from a single unknown true fish
177 accumulation rate (denoted here as X). Through this joint approach, we can estimate: the
178 aerosolization factor (η ; the magnitude of water eDNA transferred to air), the effectiveness and
179 reliability of different passive air filtering techniques (τ), and the replicability of various filters
180 (ρ) throughout the 6-week peak coho salmon spawning period.

181 We model the upstream migration of coho salmon (*Oncorhynchus kisutch*) as arising from the
182 inferred unknown true density of fish. As individuals move upriver, fish accumulate in a holding
183 area immediately downstream of the hatchery river dam. At discrete times t , the hatchery staff
184 opens the ladder gate to allow passage into holding tanks. Between successive gate-opening
185 events (Δt), additional coho salmon arrive and join the backlog in the holding area, increasing
186 the number of individuals awaiting passage. Let X represent the true daily accumulation rate
187 (also fish density at the river dam) in units of fish/day at time t , and E denote the number of days
188 elapsed between consecutive gate openings ($E_t = \Delta t$; hence $E_{t=1} = 0$). Prior to each gate
189 opening (at time t), the crew conducts a visual count N_t of accumulated fish. Assuming X_t
190 remains relatively constant between successive gate-opening events (Δt), we model the observed
191 fish counts as a Negative Binomial process:

192
$$\lambda_t = X_t \cdot E_t \quad (1)$$

193
$$N_t \sim \text{Negative Binomial}(\lambda_t, \phi) \quad (2)$$

194 where, N is the visually observed number of fish at time t , λ_t is the expected number of fish
195 accumulated over the E_t -day interval with a fixed overdispersion parameter shared across time
196 points ($\phi = 20$; hence variance $\lambda + \frac{\lambda}{\phi}$) (7, 35)

197 **Molecular process model**

198 Let W be the unobserved eDNA concentration (copies/L) in the water at time t and let ω be the
199 “integrated eDNA factor” – the conversion factor between X and W (see (7) for further
200 interpretation of this parameter). We can express the relation between the fish density and water
201 eDNA concentration as:

202
$$W_t = X_t \cdot \omega \quad (3)$$

203 Let A be the unobserved eDNA concentration (copies/day/cm²) in the air at time t that is filtered
204 using passive collection method j . We model the air eDNA concentration as a log-linear function
205 of the water eDNA with intercept η , slope = 1, and error term ε (unexplained variability; time
206 and filter specific):

207
$$\ln(A_{tj}) = \eta_j + \ln(W_t) + \varepsilon_{tj} \quad (4)$$

208 Here the intercept η can be interpreted as the water-to-air transferability (or dilution) factor and ε
 209 as the error term parameter (similar to the sum of squares error) from a linear regression where
 210 $\varepsilon_{tj} \sim \mathcal{N}(0, \tau_j)$.

211 For some filter types j (PTFE filters ($j = P$); gelatin filters ($j = G$)) we sampled two biological
 212 replicates and we used the mean of those biological replicates to determine the average
 213 concentration in the air A at time t as following:

$$214 \quad \ln(A_{tjb}) = \ln(A_{tj}) + \delta_{tjb} \quad \text{for } j \in \{P, G\} \quad (5)$$

215 where δ_b indicates the deviation of individual biological replicate from the average concentration
 216 (A_{tj}), following a normal distribution with mean 0, $\delta_{tjb} \sim \mathcal{N}(0, \rho_j)$, with ρ_j indicating the
 217 magnitude of the replicates deviation from the mean sample. Because we have only two
 218 replicates at each sampled time, we impose a sum to zero constraint on the replicates (b)
 219 collected from a single sampling time ($\sum_b \delta_{tj} = 0$).

220 To estimate the levels of eDNA concentration in water (W) and air (A), we make use of the
 221 qPCR observation models (as described in (36, 37), with slight modifications). The model
 222 compartment uses the standard curve samples to estimate the intercept (ϕ, β_0, γ_0) and slope
 223 (β_1, γ_1) parameters between the known concentration (K) and the observed data (Z and Y) from
 224 qPCR machine as follows:

$$225 \quad Z_{kr} \sim \text{Bernoulli}(\psi_k) \quad (6)$$

$$\psi_k = 1 - \exp(-K_k \cdot \theta) \quad (7)$$

$$Y_{kr} \sim \text{Normal}(\mu_k, \sigma_k) \quad \text{if } Z_{kr} = 1 \quad (8)$$

$$\mu_k = \beta_0 + \beta_{1p} \cdot \ln(K_k) \quad (9)$$

$$\sigma_k = \exp(\gamma_0 + \gamma_1 \cdot \ln(K_k)) \quad (10)$$

226 where Z is the binary outcome of target amplification for sample (k) and technical replicate (r)
 227 being present (1) or absent (0) following a Bernoulli distribution given the probability of
 228 detection ψ for each sample (k). The parameter ϕ is the intercept of the function between
 229 probability of detection ψ and the known DNA concentration (K ; copies/ μL reaction) as the
 230 predictor variable. Additionally, for equations 8-10, Y is the observed cycle threshold (Ct) for
 231 sample (k) and technical replicate (r) which follows a normal distribution with mean μ (mean
 232 Ct) and standard deviation σ for each sample (k). We model μ as a linear function of known
 233 eDNA concentration (K) with intercept β_0 and plate specific (p) slope β_1 and the standard
 234 deviation σ of the observed Y as an exponential function of known eDNA concentration with
 235 intercept γ_0 and slope γ_1 .

236 Subsequently, we build the same model compartment for estimating eDNA concentration in
 237 water and air by substituting U_t and Q_{tj} (and Q_{tjb} for $j \in \{P, G\}$) respectively, with K_k through
 238 equation 6-10 (see [SI Appendix, Fig. S1](#)), where U and Q are concentration normalized per
 239 reaction volume ($V = 10\mu\text{L}$) and surface area ($S = 16 \text{ cm}^2$ for gelatin, PTFE, and MCE, and 750
 240 cm^2 for the open containers of deionized water) of W and A respectively as follows:

241

$$U_t = \frac{W_t}{V_{itp}} \quad (11)$$

$$Q_{tjb} = A_{tjb} \cdot \frac{S_{tj}}{V_{tjbrp}} \quad (12)$$

242 The intercept and slope parameters (from equation 7, 9, and 10) between qPCR observations and
243 eDNA concentration of water, air and the standard samples are shared between model
244 compartments.

245 **Model conditions**

246 The joint model ([SI Appendix, Fig. S1](#)) was implemented using the Stan language as
247 implemented in R (package: Rstan) running four independent MCMC chains using 5000 warm-
248 up and 5000 sampling iterations (for parameters and their prior distribution see [SI Appendix,](#)
249 [Table S1](#)). The posterior predictions were diagnosed using statistics (Gelman and Rubin 1992)
250 and considered convergence for values less than 1.05 and effective sample size (ESS) greater
251 than 1000 for all parameters.

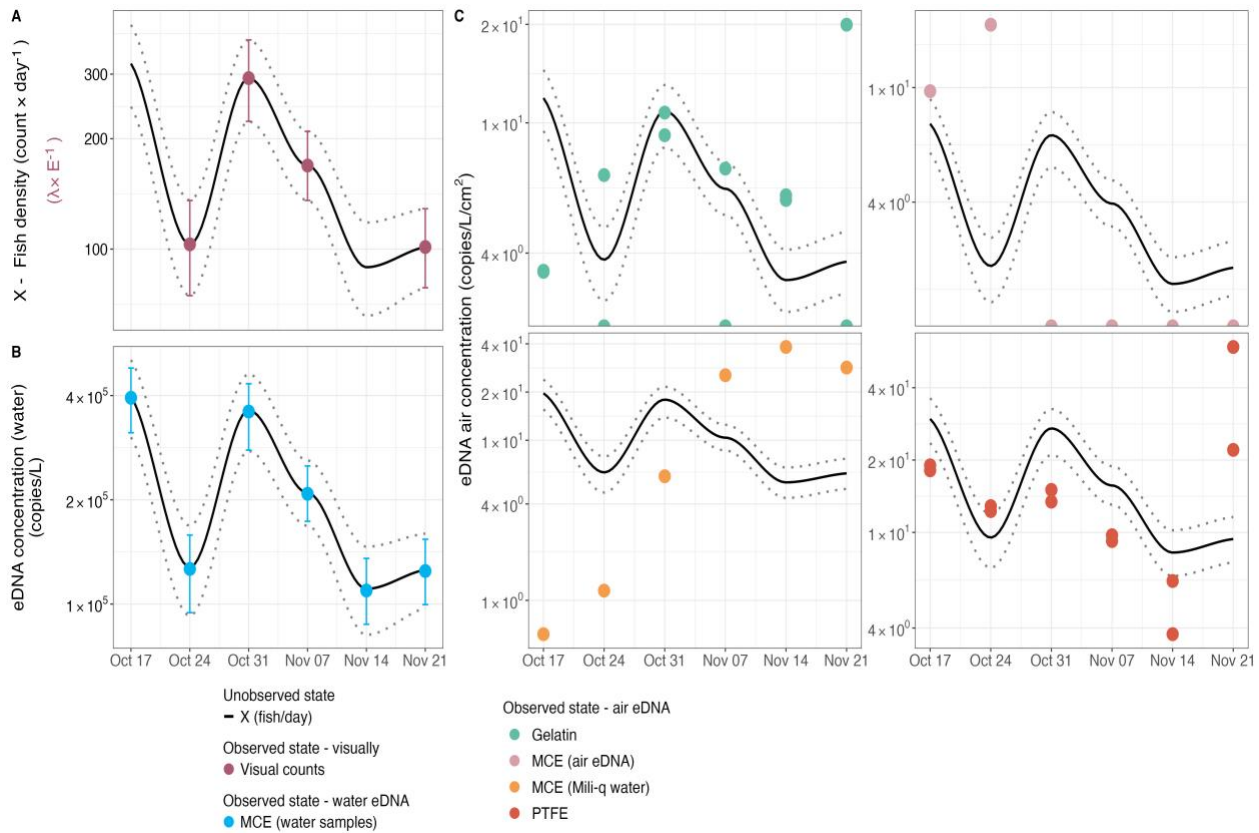
252 **Results**

253 Airborne eDNA passively detected Coho salmon and closely mirrored their abundance in the
254 river during the upstream migration period. Detection efficiency and signal strength varied
255 considerably among the different passive airborne eDNA capture methods.

256 **Fish accumulation based on visual counts and eDNA in river water**

257 Coho salmon migration occurs not as a single continuous event, but rather as a series of distinct
258 burst peaks from mid-October through late November, where the peaks are highly likely to be
259 connected with environmental factors such as water temperature and discharge. The average
260 daily accumulation rate (X; black line in Figure 2) was estimated at 160.4 fish/day with peaks
261 exceeding up to 286 fish/day and low activity of ca. 78 fish/day (Figure 2).

262 Because both observation methods (river water eDNA and visual observation) are jointly used to
263 estimate the daily accumulation rate (X), their concordance was best evaluated through the
264 parameter ω . A converged and narrowly distributed ω parameter indicates strong agreement
265 between the two methods and simultaneously a reliable conversion parameter from fish/day to
266 eDNA copies/L. In this case, $\omega = 9.578$ (95% quantile range of 9.352 to 9.804; ([SI Appendix,](#)
267 [Fig. S4](#))), suggesting consistent concordance between observed fish counts and eDNA
268 concentrations hence, biologically, this implies that an accumulation rate of 1 fish/day
269 corresponds to approximately 15000 (± 3000) copies/L.



270

271 *Figure 2: The temporal dynamics of estimated fish density in units of fish/day (X; black line with 95*
 272 *confidence intervals - dotted lines) from October 17th to November 21st compared to the posterior*
 273 *distributions of visual observations (A), eDNA concentrations (copies/L) in water (B), and eDNA*
 274 *concentrations (copies/day/cm²) in air using various filter types (C).*

275 Air eDNA signals

276 Airborne eDNA originating from coho salmon was successfully detected across all passive air
 277 collection methods deployed (gelatin, PTFE, MCE filters suspended in air, and open containers
 278 of deionized water - MCE DI water). These results provide compelling proof-of-concept
 279 evidence that genetic material from aquatic organisms can be recovered from the atmosphere
 280 without requiring active airflow systems, thereby demonstrating the viability of fully passive
 281 sampling approaches for detecting airborne aquatic eDNA under field conditions.

282 All filter types demonstrated that airborne eDNA concentrations were approximately $e^{-10.21}$
 283 ($\bar{\eta} = 10.21$) lower than corresponding waterborne eDNA concentrations, establishing a
 284 quantifiable dilution factor between water and air matrices. On average 1 copies/day/cm²
 285 captured in air is equivalent to ca. 25,000 copies/L in water. Despite the general consistency in
 286 estimating the water-to-air dilution coefficient, method-specific variations in collection
 287 efficiency were observed (Table 1; SI Appendix, Fig. S2A). PTFE filters exhibited higher capture
 288 efficiencies, collecting 2 times more eDNA than the mean across all air sampling methods (Table
 289 1). Deionized water tray (MCE DI water) demonstrated the second highest efficiency (1.3 times
 290 the average; Table 1), while gelatin filters and air suspended MCE filters showed comparatively
 291 lower capture efficacy (0.8 and 0.5 times the average, respectively; Table 1).

292 In terms of alignment with the biological activity, PTFE and gelatin filters best mirrored the
293 daily fish accumulation patterns, exhibiting the lowest residual error magnitude (expressed as the
294 standard deviation of ε) with $\tau = 0.473$ and 0.570 , respectively (Table 1; SI Appendix, Fig. S2B).
295 Conversely, MCE DI water, despite having the largest surface area, showed less agreement with
296 the fish migration dynamics ($\tau = 1.780$; Table 1; SI Appendix, Fig. S2B). The MCE air
297 suspended filters performed least effectively in tracking temporal migration patterns, failing to
298 amplify coho salmon DNA beyond the first two weeks of the sampling campaign Figure 2C.

299 Subsequently, biological replicates for gelatin and PTFE filters revealed additional insights
300 regarding methodological robustness and reproducibility. PTFE filters produced the most
301 consistent quantifications, with lower variance (expressed as the standard deviation of δ)
302 between replicates ($\rho = 0.154$; Table 1; SI Appendix, Fig. S2C), whereas gelatin filters showed a
303 higher degree of variability ($\rho = 0.386$; Table 1; SI Appendix, Fig. S2C), indicating reduced
304 reproducibility of quantitative outcomes.

305 In sum, these performance differences across sampling methods likely reflect inherent physical
306 and operational characteristics of each filter type and collection method, which in turn influence
307 their ability to capture either discrete or cumulative biological signals from the source species.

308

309 *Estimated posterior means of dilution parameter (η), standard deviation of the residuals
310 (τ), biological replicability (ρ), and capturing efficiency ($e^{(\eta-\bar{\eta})}$)*

Filter type	Dilution (in \log_e)	Standard deviation	Biological rep. error magnitude	Capturing efficiency
	(η)	(τ)	(ρ)	$e^{(\eta-\bar{\eta})}$
Gelatin	-10.45	0.473	0.386	0.785
PTFE	-9.53	0.570	0.154	1.979
MCE Air	-10.91	0.949	-	0.496
MCE DI water	-9.95	1.780	-	1.295

311

312 Model diagnostics

313 Convergence and reliability of the Bayesian model were assessed through comprehensive
314 diagnostics. All parameters (SI Appendix, Table S1) exhibited reliable Gelman-Rubin
315 convergence statistics ($\hat{R} < 1.01$) and effective sample sizes (ESS) exceeding 1000 per
316 parameter, indicating successful convergence and efficient mixing of the six independent chains
317 (SI Appendix, Fig. S3A).

318 No divergent transitions were detected during sampling, and the maximum tree depth was not
319 exceeded, indicating no issues with divergence or exploration limits (SI Appendix, Fig. S3B).
320 The posterior likelihood demonstrated convergence before the sampling phase began, with all
321 chains exhibiting high mixing, confirming robust exploration of the parameter space (SI
322 Appendix, Fig. S3B).

323 Prior sensitivity analyses revealed that posterior estimates differed from priors, demonstrating
324 that the posteriors were appropriately updated based on the observed data rather than being
325 heavily influenced by prior assumptions (SI Appendix, Fig. S4). Additionally, the posterior
326 predictive checks (PPC) demonstrated that the model reliably reproduced the observed data,
327 supporting the validity of parameter estimates (SI Appendix, Fig. S5).

328 Collectively, these diagnostics confirm the reliability and validity of the Bayesian model used
329 here.

330 Discussion

331 A New Dimension of Biodiversity Monitoring

332 Our study establishes, for the first time, that passive airborne eDNA sampling can reliably
333 capture and track molecular signals from aquatic organisms. This represents a paradigm shift in
334 how we access aquatic biodiversity—through the air, without ever touching the water. In
335 salmon-spawning streams, genetic material from the river is transported into the air likely by
336 evaporation, bubble-burst aerosolization at riffles and splashes, and the rigorous churning of
337 spawning fish (38, 39). Collections from multiple passive samplers, when compared with
338 conventional water-based eDNA assays and daily visual counts, reveal a clear and quantitative
339 relationship between airborne eDNA concentration and salmon density.

340 Until now, airborne eDNA surveys have reported fish or other strictly aquatic taxa as likely to be
341 laboratory contamination, zoo-feed artifacts, or piscivore fecal bioaerosols (15–18). Our data
342 suggest otherwise: this is a real ecological signal rather than an experimental artifact. It is likely
343 that wind speed, relative humidity, and temperature will determine how far and how long
344 aerosolized aquatic eDNA will travel before being redeposited (40, 41). For example, high
345 humidity and rainfall force rapid settling and very localized deposition while dry, windy
346 conditions might carry genetic plumes further distances downwind (42, 43). These
347 environmental controls, combined with air currents above riffles and splashes, should be
348 considered when determining how passive samplers capture transient pulses of biological
349 activity.

350 Sampler Design Shapes Signal Detection

351 Over 24-hour deployments, vertically oriented gelatin and PTFE filters acted as higher-resolution
352 “fish-activity” samplers (44). Ambient air currents likely swept fine, splash-generated aerosols
353 rich in salmon DNA onto their membranes, producing yields that rose and fell in sync with live
354 fish counts and water-eDNA levels (45). In contrast, the large horizontal tray of deionized water
355 seemed to function more like a hydraulic-driven deposition trap. The tray saw a steady
356 accumulation of eDNA over the six weeks and thus could have been collecting more coarse
357 spray, foam, and decay-derived particulates from river turbulence and from decomposing
358 carcasses (39, 46). Because salmon carcasses often remain in shallow banks and backwaters as
359 the spawning season progresses, it is plausible that river turbulence and discharge could generate
360 larger droplets over decomposing tissue, potentially facilitating eDNA dispersal (38, 47). These
361 coarse droplets settle rapidly and dominate deposition on horizontal collectors while the fine
362 fraction produced by active fish movement is under-represented. Gelatin and PTFE filters thus

363 seem to provide snapshots of biologically driven eDNA flux whereas the water tray seemed to
364 integrate both flow-driven and decay-driven inputs into a steadily rising accumulation curve.

365 The filter materials and operational context also shaped the air sampling performance. PTFE
366 filters, known for their durability, delivered the most consistent results of all the passive filtration
367 methods; gelatin filters yielded the highest sensitivity but showed greater variability; mixed
368 cellulose ester filters captured negligible airborne DNA; and the open tray, with roughly 50 times
369 more surface area than the vertical filters, recovered the highest total DNA yield. These samplers
370 respond differently to weather. PTFE filters are generally unaffected by rain, whereas gelatin
371 filters perform best in dry conditions because they dissolve when wet. Rainfall also introduces a
372 trade-off for the tray: heavy rain can dilute the accumulated eDNA but may also scour additional
373 airborne or splash-borne DNA into the water. Real-world debris, such as leaves, insects,
374 sediment, can also wash into the tray, increasing the risk of clogging or necessitating pre-
375 filtration before DNA extraction. Although our sample size is too small to quantify these
376 opposing effects, future work should explicitly test how precipitation intensity influences both
377 concentration and total yield (12).

378 Air is Dilute Water: Balancing Capture and Decay

379 On average, our data showed that eDNA in the air was roughly 25,000 times less concentrated
380 than in the water, at a level that approaches the lower limits of qPCR detection. Despite this
381 extreme dilution, our rigorous sampling, laboratory methods, and statistical models reliably
382 picked up those sparse molecules, obtaining consistent, quantitative signals across the entire
383 spawning season. To put this in perspective, dissolving a teaspoon of salt into a large aquarium
384 yields a similar dilution magnitude: only a tiny fraction of shed DNA ever makes it into the
385 overlying air, yet those few copies suffice to track real-time salmon activity. In particular,
386 vertically oriented filters intercepted transient eDNA peaks that rose and fell in concert with
387 visual counts, demonstrating that even at extreme dilution, airborne eDNA can still capture fine
388 scale changes in fish presence that reflects real-world population dynamics.

389 Longer passive-sampler deployments naturally accumulate more settled eDNA, but they also
390 expose collected material to ultraviolet radiation, microbial degradation and fluctuating
391 humidity, all of which erode DNA integrity over time (48). (49) showed that waterborne eDNA
392 degrades with a half-life of hours to days under natural sunlight and microbial loads, suggesting
393 that once deposited, airborne fragments may decay on comparable or even faster timescales. By
394 contrast, (17) found that passive air particle collections continued to accrue new species
395 detections for up to 96 hours, without specifying when deposition begins to be outpaced by
396 degradation. In practical terms, this means that in a week-long deployment much of the DNA
397 captured from early days may have degraded long before retrieval, so that the majority of signal
398 reflects material deposited in the final one or two days of sampling. We therefore selected a
399 24-hour deployment to capture transient eDNA plumes while limiting post-deposition loss(12).
400 Future work should vary deployment lengths from a few hours to several days, and pair them
401 with controlled decay assays, for example by spiking synthetic DNA onto filters and tracking its
402 persistence, to determine the point at which accumulation and degradation balance.

403 Our findings also agree with the recent work by (44) who showed that passive air samplers
404 outperform active pumps by sampling intermittent, DNA-rich plumes over long intervals and
405 detecting greater species richness. In our streams, vertical filters captured transient bursts of

406 salmon eDNA in near real-time, while the open tray, and likely longer deployments, would tend
407 to smooth those peaks into an integrated signal. Contrastingly, active-pump systems operating
408 for only hours would average across plumes and risk overlooking fine-scale temporal changes.

409 By systematically mapping this interplay between deposition and degradation, and by
410 benchmarking passive against active approaches, we can establish best-practice guidelines for
411 airborne eDNA sampling durations. This effort would mirror how water-based eDNA workflows
412 define optimal filtration volumes and storage times (20, 50) and would enable robust,
413 context-specific deployments that maximize genuine signal recovery for real-time biodiversity
414 monitoring.

415 **Minimal Tools, Maximum Reach and Navigating Limitations**

416 Perhaps most striking result from our work is the simplicity and versatility of passive airborne
417 sampling. No pumps or power are needed, and equipment is extremely low cost and easy to
418 deploy. This minimal-infrastructure approach makes it viable for remote headwaters, steep
419 mountain channels, urban stormwater networks, and contaminated waters where sampling is
420 unsafe (51, 52). By integrating visual surveys, water-based eDNA and airborne eDNA, we
421 establish a biomonitoring framework that is non-invasive, scalable and low-impact. In an era of
422 intensifying droughts, floods and public-health risks such as bacterial outbreaks in stagnant
423 waters, airborne eDNA offers resilient pathways for rapid invasive-species alerts, real-time
424 disease surveillance in flood-prone wetlands and non-invasive population censuses in protected
425 spawning grounds.

426 Naturally, challenges remain. Passive deployments rely on surface-area-by-time metrics rather
427 than standardized air-volume units, complicating direct comparisons across studies. Optimal
428 exposure times must balance accumulation against DNA degradation from UV, microbes and
429 moisture (48). Weather variability in wind, humidity and rain can alter deposition rates and
430 sampler efficiency (12, 21). Future work should refine sampler design, systematically compare
431 vertical and horizontal orientations, explore automated or drone-based retrieval and integrate
432 river discharge and meteorological data into quantitative models (38, 42, 53, 54).

433 Our study begins to chart a portion of airborne eDNA ecology's in five key dimensions (21). We
434 confirm origin by matching airborne DNA trends to co-occurring water eDNA and fish counts.
435 We elucidate transport mechanisms such as evaporation, bubble bursts and fish activity. We
436 quantify dispersal and dilution by measuring a 25,000-times concentration difference between
437 water and air samples. We demonstrate fate through differential deposition on vertical filters and
438 horizontal trays. Finally, we show that airborne DNA fragments remain amplifiable, offering an
439 initial glimpse into their molecular state after transport. These insights lay the groundwork for
440 future studies on persistence, degradation and particle-size distributions from airborne eDNA
441 (55).

442 Overall, our work overturns the assumption that aquatic eDNA belongs solely underwater. By
443 demonstrating that genetic signals from fish and other aquatic life routinely escape into and can
444 be captured from the air, we open a new paradigm for ecological monitoring. The atmosphere
445 above water emerges as a reliable, quantifiable reservoir of biodiversity data. This advance
446 promises transformative applications from invasive species alerts in drought-stricken reservoirs

447 to pathogen surveillance in flood-prone wetlands and non-invasive censuses in protected streams,
448 equipping managers with a resilient, real-time window into aquatic ecosystems.

449 **Acknowledgments**

450 We thank Natasha Kacoroski, Larry Franks, and the dedicated volunteers at Friends of the
451 Issaquah Salmon Hatchery for their generous support in the field. We are also grateful to Travis
452 A. Burnett and Darin Combs at the Washington Department of Fish and Wildlife for facilitating
453 access and permitting field experimental work at the Issaquah Hatchery. Additional thanks to
454 Pedro F.P. Brandão-Dias for assistance with air filter deployments, and to Kevan Yamanaka at
455 the Monterey Bay Aquarium Research Institute for fabricating the 3D-printed passive filter
456 holders. We are especially grateful to Chris Sergeant for valuable insights on salmon biology that
457 shaped the interpretation of our findings, and to Ole Shelton for statistical advice that improved
458 our analytical approach. We acknowledge funding support from the Packard Foundation [Grant
459 No. GR016745].

460 **Author contributions**

461 Y.C.A.I. conceived the study. Y.C.A.I. G.G and E.A.A. designed the field and laboratory
462 protocols. Y.C.A.I. and G.G. jointly designed the downstream statistical analyses and Bayesian
463 modeling framework. G.G. conducted all statistical analyses, with inputs from R.P.K. The
464 fieldwork was performed by Y.C.A.I. and E.A.A., while Y.C.A.I. and G.G. co-wrote the
465 manuscript. R.P.K. supervised the project, contributed to conceptual guidance, and provided
466 critical revisions. All authors contributed to the study design and approved the final manuscript.

467 **Data availability**

468 The authors declare that they have no competing interests. All data needed to evaluate the
469 conclusions in this paper are available in the main text and/or the Supplementary Materials.
470 Codes are available on <https://github.com/gledguri/Air-eDNA-quant>. Additional data, code, and
471 materials will be made available upon reasonable request. No materials were subject to material
472 transfer agreements (MTAs).

- 473 1. D. Dudgeon, A. H. Arthington, M. O. Gessner, Z. Kawabata, D. J. Knowler, C. Lévéque, R. J. Naiman, A.
474 Prieur-Richard, D. Soto, M. L. J. Stiassny, C. A. Sullivan, [Freshwater biodiversity: Importance, threats, status and](#)
475 [conservation challenges](#). *Biological Reviews* **81**, 163–182 (2006).
- 476 2. A. J. Reid, A. K. Carlson, I. F. Creed, E. J. Eliason, P. A. Gell, P. T. J. Johnson, K. A. Kidd, T. J.
477 MacCormack, J. D. Olden, S. J. Ormerod, J. P. Smol, W. W. Taylor, K. Tockner, J. C. Vermaire, D. Dudgeon, S. J.
478 Cooke, [Emerging threats and persistent conservation challenges for freshwater biodiversity](#). *Biological Reviews* **94**,
479 849–873 (2019).
- 480 3. J. Biggs, N. Ewald, A. Valentini, C. Gaboriaud, T. Dejean, R. A. Griffiths, J. Foster, J. W. Wilkinson, A.
481 Arnell, P. Brotherton, P. Williams, F. Dunn, [Using eDNA to develop a national citizen science-based monitoring](#)
482 [programme for the great crested newt \(*Triturus cristatus*\)](#). *Biological Conservation* **183**, 19–28 (2015).
- 483 4. A. C. Thomas, S. Tank, P. L. Nguyen, J. Ponce, M. Sinnesael, C. S. Goldberg, [A system for rapid eDNA](#)
484 [detection of aquatic invasive species](#). *Environmental DNA* **2**, 261–270 (2020).

- 485 5. S. P. Wilkinson, A. A. Gault, S. A. Welsh, J. P. Smith, B. O. David, A. S. Hicks, D. R. Fake, A. M. Suren,
486 M. R. Shaffer, S. N. Jarman, M. Bunce, [TICI: A taxon-independent community index for eDNA-based ecological](#)
487 [health assessment](#). *PeerJ* **12**, e16963 (2024).
- 488 6. E. A. Allan, R. P. Kelly, E. R. D'Agnese, M. N. Garber-Yonts, M. R. Shaffer, Z. J. Gold, A. O. Shelton,
489 [Quantifying impacts of an environmental intervention using environmental DNA](#). *Ecological Applications* **33**, e2914
490 (2023).
- 491 7. G. Guri, A. O. Shelton, R. P. Kelly, N. Yoccoz, T. Johansen, K. Præbel, T. Hanebrekke, J. L. Ray, J. Fall,
492 [Predicting trawl catches using environmental DNA](#). *ICES Journal of Marine Science* **81**, 1536–1548
493 (2024).
- 494 8. M. D. Tillotson, R. P. Kelly, J. J. Duda, M. Hoy, J. Kralj, T. P. Quinn, [Concentrations of environmental](#)
495 [DNA \(eDNA\) reflect spawning salmon abundance at fine spatial and temporal scales](#). *Biological Conservation* **220**,
496 1–11 (2018).
- 497 9. E. L. Clare, C. K. Economou, C. G. Faulkes, J. D. Gilbert, F. Bennett, R. Drinkwater, J. E. Littlefair,
498 [eDNAir: Proof of concept that animal DNA can be collected from air sampling](#). *PeerJ* **9**, e11030 (2021).
- 499 10. N. R. Garrett, J. Watkins, N. B. Simmons, B. Fenton, A. Maeda-Obregon, D. E. Sanchez, E. M. Froehlich,
500 [F. M. Walker, J. E. Littlefair, E. L. Clare, Airborne eDNA documents a diverse and ecologically complex tropical](#)
501 [bat and other mammal community](#). *Environmental DNA* **5**, 350–362 (2023).
- 502 11. M. D. Johnson, R. D. Cox, M. A. Barnes, [Analyzing airborne environmental DNA: A comparison of](#)
503 [extraction methods, primer type, and trap type on the ability to detect airborne eDNA from terrestrial plant](#)
504 [communities](#). *Environmental DNA* **1**, 176–185 (2019).
- 505 12. M. D. Johnson, M. A. Barnes, N. R. Garrett, E. L. Clare, [Answers blowing in the wind: Detection of birds,](#)
506 [mammals, and amphibians with airborne environmental DNA in a natural environment over a yearlong survey](#).
507 [Environmental DNA](#) **5**, 375–387 (2023).
- 508 13. C. Lynggaard, T. G. Frøslev, M. S. Johnson, M. T. Olsen, K. Bohmann, [Airborne environmental DNA](#)
509 [captures terrestrial vertebrate diversity in nature](#). *Molecular Ecology Resources* **24**, e13840 (2024).
- 510 14. F. Roger, H. R. Ghanavi, N. Danielsson, N. Wahlberg, J. Löndahl, L. B. Pettersson, G. K. S. Andersson, N.
511 Boke Olén, Y. Clough, [Airborne environmental DNA metabarcoding for the monitoring of terrestrial insects—A](#)
512 [proof of concept from the field](#). *Environmental DNA* **4**, 790–807 (2022).
- 513 15. C. Lynggaard, M. F. Bertelsen, C. V. Jensen, M. S. Johnson, T. G. Frøslev, M. T. Olsen, K. Bohmann,
514 [Airborne environmental DNA for terrestrial vertebrate community monitoring](#). *Current Biology* **32**, 701–707.e5
515 (2022).
- 516 16. A. R. Sullivan, E. Karlsson, D. Svensson, B. Brindefalk, J. A. Villegas, A. Mikko, D. Bellieny, A. B.
517 Siddique, A.-M. Johansson, H. Grahn, D. Sundell, A. Norman, P.-A. Esseen, A. Sjödin, N. J. Singh, T. Brodin, M.
518 Forsman, P. Stenberg, [Airborne eDNA captures three decades of ecosystem biodiversity \(2023\).](#)
519 <https://doi.org/10.1101/2023.12.06.569882>.
- 520 17. M. J. Klepke, E. E. Sigsgaard, M. R. Jensen, K. Olsen, P. F. Thomsen, [Accumulation and diversity of](#)
521 [airborne, eukaryotic environmental DNA](#). *Environmental DNA* **4**, 1323–1339 (2022).
- 522 18. C. Lynggaard, S. Calvignac-Spencer, C. A. Chapman, U. Kalbitzer, F. H. Leendertz, P. A. Omeja, E. A.
523 Opito, D. Sarkar, K. Bohmann, J. F. Gogarten, [Vertebrate environmental DNA from leaf swabs](#). *Current Biology* **33**,
524 R853–R854 (2023).

- 525 19. O. Tournayre, J. E. Littlefair, N. R. Garrett, J. J. Allerton, A. S. Brown, M. E. Cristescu, E. L. Clare, First
526 national survey of terrestrial biodiversity using airborne eDNA (2025). <https://doi.org/10.1101/2025.04.07.647580>.
- 527 20. F. Altermatt, M. Couton, L. Carraro, F. Keck, L. Lawson-Handley, F. Leese, X. Zhang, Y. Zhang, R. C.
528 Blackman, Utilizing aquatic environmental DNA to address global biodiversity targets. *Nature Reviews Biodiversity*,
529 doi: [10.1038/s44358-025-00044-x](https://doi.org/10.1038/s44358-025-00044-x) (2025).
- 530 21. M. Johnson, M. A. Barnes, *Microbial airborne environmental DNA analysis: A review of progress,
531 challenges, and recommendations for an emerging application*. *Molecular Ecology Resources* **24**, e13998 (2024).
- 532 22. C. Folke, S. Polasky, J. Rockström, V. Galaz, F. Westley, M. Lamont, M. Scheffer, H. Österblom, S. R.
533 Carpenter, F. S. Chapin, K. C. Seto, E. U. Weber, B. I. Crona, G. C. Daily, P. Dasgupta, O. Gaffney, L. J. Gordon,
534 H. Hoff, S. A. Levin, J. Lubchenco, W. Steffen, B. H. Walker, *Our future in the Anthropocene biosphere*. *Ambio* **50**,
535 834–869 (2021).
- 536 23. E. C. Monahan, D. E. Spiel, K. L. Davidson, “*A model of marine aerosol generation via whitecaps and
537 wave disruption*” in *Oceanic Whitecaps*, E. C. Monahan, G. M. Niocaill, Eds. (Springer, Dordrecht, 1986) vol. 2 of
538 *Oceanographic sciences library*.
- 539 24. J. H. Seinfeld, S. N. Pandis, *Atmospheric Chemistry and Physics: From Air Pollution to Climate Change*
540 (Wiley, ed. 3, 2016).
- 541 25. L. Duchemin, S. Popinet, C. Josserand, S. Zaleski, *Jet formation in bubbles bursting at a free surface*.
542 *Physics of Fluids* **14**, 3000–3008 (2002).
- 543 26. R. P. Mueller, S. S. Southard, C. W. May, W. H. Pearson, V. I. Cullinan, *Juvenile Coho Salmon Leaping
544 Ability and Behavior in an Experimental Culvert Test Bed*. *Transactions of the American Fisheries Society* **137**,
545 941–950 (2008).
- 546 27. E. Stell, J. J. Hoover, L. Fuller, G. R. Parsons, *Analyzing Leap Characteristics and Water Escape Velocities
547 of Silver Carp Using In Situ Video Analysis*. *North American Journal of Fisheries Management* **40**, 163–174
548 (2020).
- 549 28. A. I. J. M. Van Dijk, L. A. Bruijnzeel, E. H. Eisma, *A methodology to study rain splash and wash processes
550 under natural rainfall*. *Hydrological Processes* **17**, 153–167 (2003).
- 551 29. W. Chen, J. Wang, Y. Zhao, Y. He, J. Chen, C. Dong, L. Liu, J. Wang, L. Zhou, *Contrasting pollution
552 responses of native and non-native fish communities in anthropogenically disturbed estuaries unveiled by eDNA
553 metabarcoding*. *Journal of Hazardous Materials* **480**, 136323 (2024).
- 554 30. D. V. Ruiz-Ramos, R. S. Meyer, D. Toews, M. Stephens, M. K. Kolster, J. P. Sexton, *Environmental DNA
555 (eDNA) detects temporal and habitat effects on community composition and endangered species in ephemeral
556 ecosystems: A case study in vernal pools*. *Environmental DNA* **5**, 85–101 (2023).
- 557 31. J. Wan, Z. Zhang, Y. Huo, X. Wang, Y. Wang, J. Wu, M. Huo, *Particle Size Matters: Distribution, Source,
558 and Seasonality Characteristics of Airborne and Pathogenic Bacteria in Wastewater Treatment Plants*. *Atmosphere*
559 **14**, 465 (2023).
- 560 32. Y. Wu, F. Shen, M. Yao, *Use of gelatin filter and BioSampler in detecting airborne H5N1 nucleotides,
561 bacteria and allergens*. *Journal of Aerosol Science* **41**, 869–879 (2010).
- 562 33. P. Harnpicharnchai, P. Pumkaeo, P. Siriarchawatana, S. Likhitrattanapisal, S. Mayteeworakoon, L.
563 Ingsrisawang, W. Boonsin, L. Eurwilaichitr, S. Ingsriswang, *AirDNA sampler: An efficient and simple device
564 enabling high-yield, high-quality airborne environment DNA for metagenomic applications*. *PLOS ONE* **18**,
565 e0287567 (2023).

- 566 34. J. J. Duda, M. S. Hoy, D. M. Chase, G. R. Pess, S. J. Brenkman, M. M. McHenry, C. O. Ostberg,
567 **Environmental DNA is an effective tool to track recolonizing migratory fish following large-scale dam removal.**
568 *Environmental DNA* **3**, 121–141 (2021).
- 569 35. D. W. Welch, Y. Ishida, **On the Statistical Distribution of Salmon in the Sea: Application of the Negative**
570 **Binomial Distribution, and the Influence of Sampling Effort.** *Canadian Journal of Fisheries and Aquatic Sciences*
571 **50**, 1029–1038 (1993).
- 572 36. G. Guri, J. L. Ray, A. O. Shelton, R. P. Kelly, K. Præbel, E. Andruszkiewicz Allan, N. Yoccoz, T.
573 Johansen, O. S. Wangensteen, T. Hanebrekke, J.-I. Westgaard, **Quantifying the Detection Sensitivity and Precision**
574 **of QPCR and ddPCR Mechanisms for eDNA Samples.** *Ecology and Evolution* **14**, e70678 (2024).
- 575 37. A. O. Shelton, A. Ramón-Laca, A. Wells, J. Clemons, D. Chu, B. E. Feist, R. P. Kelly, S. L. Parker-Stetter,
576 R. Thomas, K. M. Nichols, L. Park, **Environmental DNA provides quantitative estimates of Pacific hake abundance**
577 **and distribution in the open ocean.** *Proceedings of the Royal Society B: Biological Sciences* **289**, 20212613 (2022).
- 578 38. Z. T. Wood, A. Lacoursière-Roussel, F. LeBlanc, M. Trudel, M. T. Kinnison, C. Garry McBrine, S. A.
579 **Pavey, N. Gagné, Spatial Heterogeneity of eDNA Transport Improves Stream Assessment of Threatened Salmon**
580 **Presence, Abundance, and Location.** *Frontiers in Ecology and Evolution* **9**, 650717 (2021).
- 581 39. K. A. Prather, T. H. Bertram, V. H. Grassian, G. B. Deane, M. D. Stokes, P. J. DeMott, L. I. Aluwihare, B.
582 P. Palenik, F. Azam, J. H. Seinfeld, R. C. Moffet, M. J. Molina, C. D. Cappa, F. M. Geiger, G. C. Roberts, L. M.
583 Russell, A. P. Ault, J. Baltrusaitis, D. B. Collins, C. E. Corrigan, L. A. Cuadra-Rodriguez, C. J. Ebbin, S. D.
584 Forestieri, T. L. Guasco, S. P. Hersey, M. J. Kim, W. F. Lambert, R. L. Modini, W. Mui, B. E. Pedler, M. J. Ruppel,
585 O. S. Ryder, N. G. Schoepp, R. C. Sullivan, D. Zhao, **Bringing the ocean into the laboratory to probe the chemical**
586 **complexity of sea spray aerosol.** *Proceedings of the National Academy of Sciences* **110**, 7550–7555 (2013).
- 587 40. N. Abrego, B. Furneaux, B. Hardwick, P. Somervuo, I. Palorinne, C. A. Aguilar-Trigueros, N. R. Andrew,
588 U. V. Babiy, T. Bao, G. Bazzano, S. N. Bondarchuk, T. C. Bonebrake, G. L. Brennan, S. Bret-Harte, C. Bässler, L.
589 Cagnolo, E. K. Cameron, E. Chapurlat, S. Creer, L. P. D'Acqui, N. De Vere, M.-L. Desprez-Loustau, M. A. K.
590 Dongmo, I. B. D. Jacobsen, B. L. Fisher, M. Flores De Jesus, G. S. Gilbert, G. W. Griffith, A. A. Gritsuk, A. Gross,
591 H. Grudd, P. Halme, R. Hanna, J. Hansen, L. H. Hansen, A. D. M. T. Hegbe, S. Hill, I. D. Hogg, J. Hultman, K. D.
592 Hyde, N. A. Hynson, N. Ivanova, P. Karisto, D. Kerdraon, A. Knorre, I. Krisai-Greilhuber, J. Kurhinen, M.
593 Kuzmina, N. Lecomte, E. Lecomte, V. Loaiza, E. Lundin, A. Meire, A. Mešić, O. Miettinen, N. Monkhouse, P.
594 Mortimer, J. Müller, R. H. Nilsson, P. Y. C. Nonti, J. Nordén, B. Nordén, V. Norros, C. Paz, P. Pellikka, D. Pereira,
595 G. Petch, J.-M. Pitkänen, F. Popa, C. Potter, J. Purhonen, S. Pätsi, A. Rafiq, D. Raharinjanahary, N. Rakos, A. R.
596 Rathnayaka, K. Raundrup, Y. A. Rebriev, J. Rikkinen, H. M. K. Rogers, A. Rogovsky, Y. Rozhkov, K. Runnel, A.
597 Saarto, A. Savchenko, M. Schlegel, N. M. Schmidt, S. Seibold, C. Skjøth, E. Stengel, S. V. Sutyrina, I. Syväperä,
598 L. Tedersoo, J. Timm, L. Tipton, H. Toju, M. Uscka-Perzanowska, M. Van Der Bank, F. H. Van Der Bank, B.
599 Vandenbrink, S. Ventura, S. R. Vignisson, X. Wang, W. W. Weisser, S. N. Wijesinghe, S. J. Wright, C. Yang, N. S.
600 Yorou, A. Young, D. W. Yu, E. V. Zakharov, P. D. N. Hebert, T. Roslin, O. Ovaskainen, **Airborne DNA reveals**
601 **predictable spatial and seasonal dynamics of fungi.** *Nature* **631**, 835–842 (2024).
- 602 41. M. Giolai, W. Verweij, S. Martin, N. Pearson, P. Nicholson, R. M. Leggett, M. D. Clark, **Measuring air**
603 **metagenomic diversity in an agricultural ecosystem.** *Current Biology* **34**, 3778–3791.e4 (2024).
- 604 42. S. Galbán, A. Justel, S. González, A. Quesada, **Local meteorological conditions, shape and desiccation**
605 **influence dispersal capabilities for airborne microorganisms.** *Science of The Total Environment* **780**, 146653 (2021).
- 606 43. T. Maki, K. Hosaka, K. C. Lee, Y. Kawabata, M. Kajino, M. Uto, K. Kita, Y. Igarashi, **Vertical distribution**
607 **of airborne microorganisms over forest environments: A potential source of ice-nucleating bioaerosols.** *Atmospheric*
608 *Environment* **302**, 119726 (2023).

- 609 44. H. Jager, K. B. Trimbos, J.-M. Luursema, A. G. C. L. Speksnijder, K. A. Stewart, A breath of fresh air:
610 Comparative evaluation of passive versus active airborne eDNA sampling strategies (2025).
611 <https://doi.org/10.1101/2025.03.26.645491>.
- 612 45. D. C. Blanchard, A. H. Woodcock, THE PRODUCTION, CONCENTRATION, AND VERTICAL
613 DISTRIBUTION OF THE SEA-SALT AEROSOL*. *Annals of the New York Academy of Sciences* **338**, 330–347
614 (1980).
- 615 46. W. C. Hinds, Y. Zhu, *Aerosol Technology: Properties, Behavior, and Measurement of Airborne Particles*
616 (John Wiley & Sons, 2022).
- 617 47. B. A. Herman, “Use of foreign eDNA tracers to resolve site- and time-specific eDNA distributions in
618 natural streams,” thesis, Humboldt State University (2023).
- 619 48. P. F. P. Brandão-Dias, D. M. C. Hallack, E. D. Snyder, J. L. Tank, D. Bolster, S. Volponi, A. J. Shogren, G.
620 A. Lamberti, K. Bibby, S. P. Egan, Particle size influences decay rates of environmental DNA in aquatic systems.
621 *Molecular Ecology Resources* **23**, 756–770 (2023).
- 622 49. K. M. Strickler, A. K. Fremier, C. S. Goldberg, Quantifying effects of UV-B, temperature, and pH on
623 eDNA degradation in aquatic microcosms. *Biological Conservation* **183**, 85–92 (2015).
- 624 50. M. A. Barnes, C. R. Turner, The ecology of environmental DNA and implications for conservation
625 genetics. *Conservation Genetics* **17**, 1–17 (2016).
- 626 51. J. B. Harrison, J. M. Sunday, S. M. Rogers, Predicting the fate of eDNA in the environment and
627 implications for studying biodiversity. *Proceedings of the Royal Society B: Biological Sciences* **286**, 20191409
628 (2019).
- 629 52. M. Bagley, E. Pilgrim, M. Knapp, C. Yoder, J. Santo Domingo, A. Banerji, High-throughput environmental
630 DNA analysis informs a biological assessment of an urban stream. *Ecological Indicators* **104**, 378–389 (2019).
- 631 53. S. Kirchgeorg, J. J. M. Chang, Y. C. A. Ip, M. Jucker, C. Geckeler, M. Lüthi, E. Van Der Loo, E. Mächler,
632 N. D. Franco-Sierra, M. A. G. Herrera, L. Pellissier, K. Deiner, A. Desiderato, S. Mintchev, eProbe: Sampling of
633 Environmental DNA within Tree Canopies with Drones. *Environmental Science & Technology* **58**, 16410–16420
634 (2024).
- 635 54. A. J. Shogren, J. L. Tank, E. Andruszkiewicz, B. Olds, A. R. Mahon, C. L. Jerde, D. Bolster, Controls on
636 eDNA movement in streams: Transport, Retention, and Resuspension. *Scientific Reports* **7**, 5065 (2017).
- 637 55. P. F. Brandao-Dias, M. Shaffer, G. Guri, K. M. Parsons, R. P. Kelly, E. A. Allan, Differential Decay of
638 Multiple eNA Components from a Cetacean (2025). <https://doi.org/10.1101/2025.05.09.653189>.

Supplementary Material
Fish from the Sky: Airborne eDNA Tracks Aquatic Life

Yin Cheong Aden Ip^{1*} Gledis Guri^{1*} Elizabeth Andruszkiewicz Allan¹
Ryan P. Kelly¹

May 23, 2025

¹ School of Marine and Environmental Affairs, University of Washington, Seattle, Washington, USA
* shared first authorship

corresponding author **adenip@uw.edu**

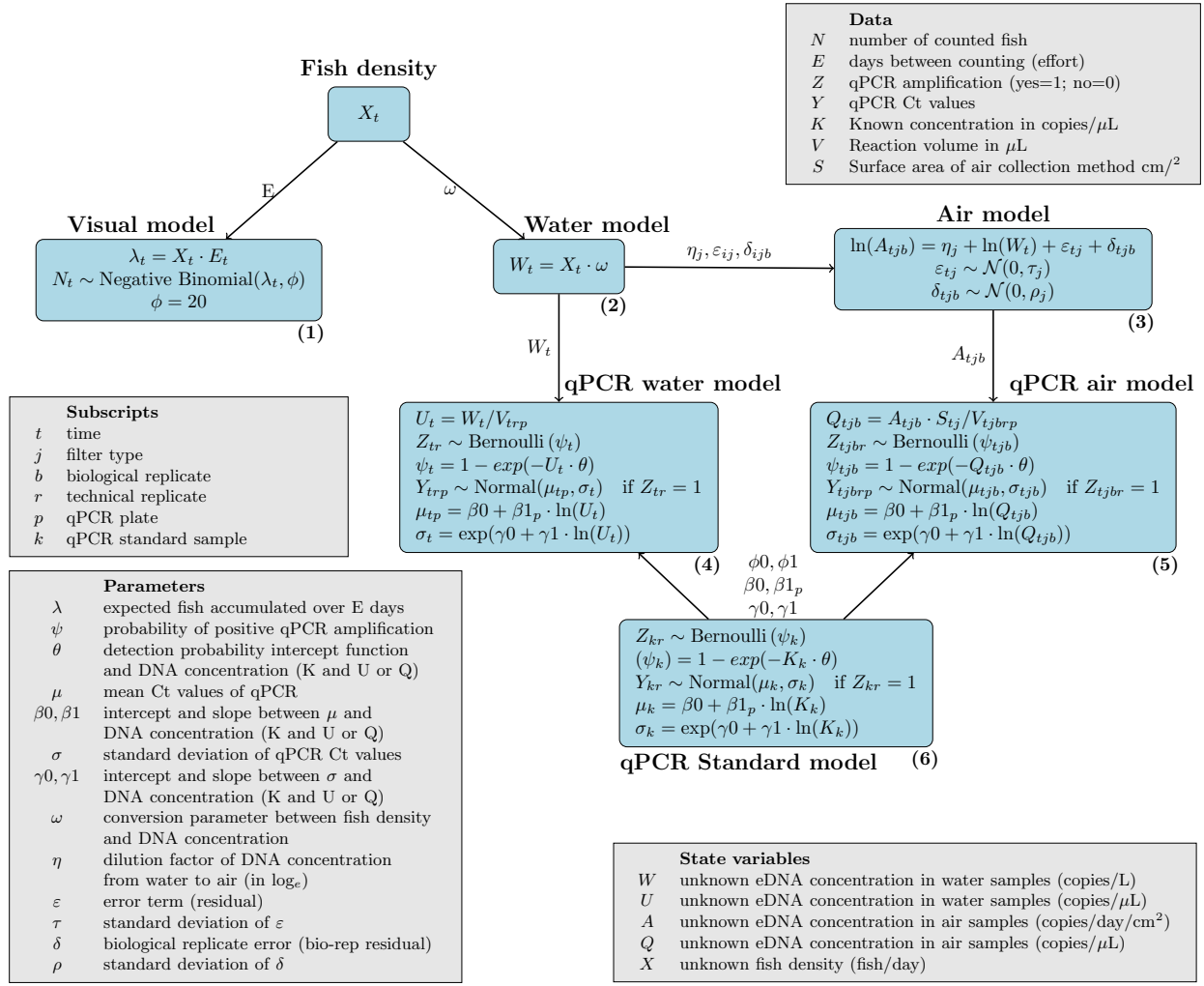


Figure 1: Directed acyclic graph (DAG) of joint Bayesian model for linking salmon migration dynamics from visual observation, water and air eDNA concentration.

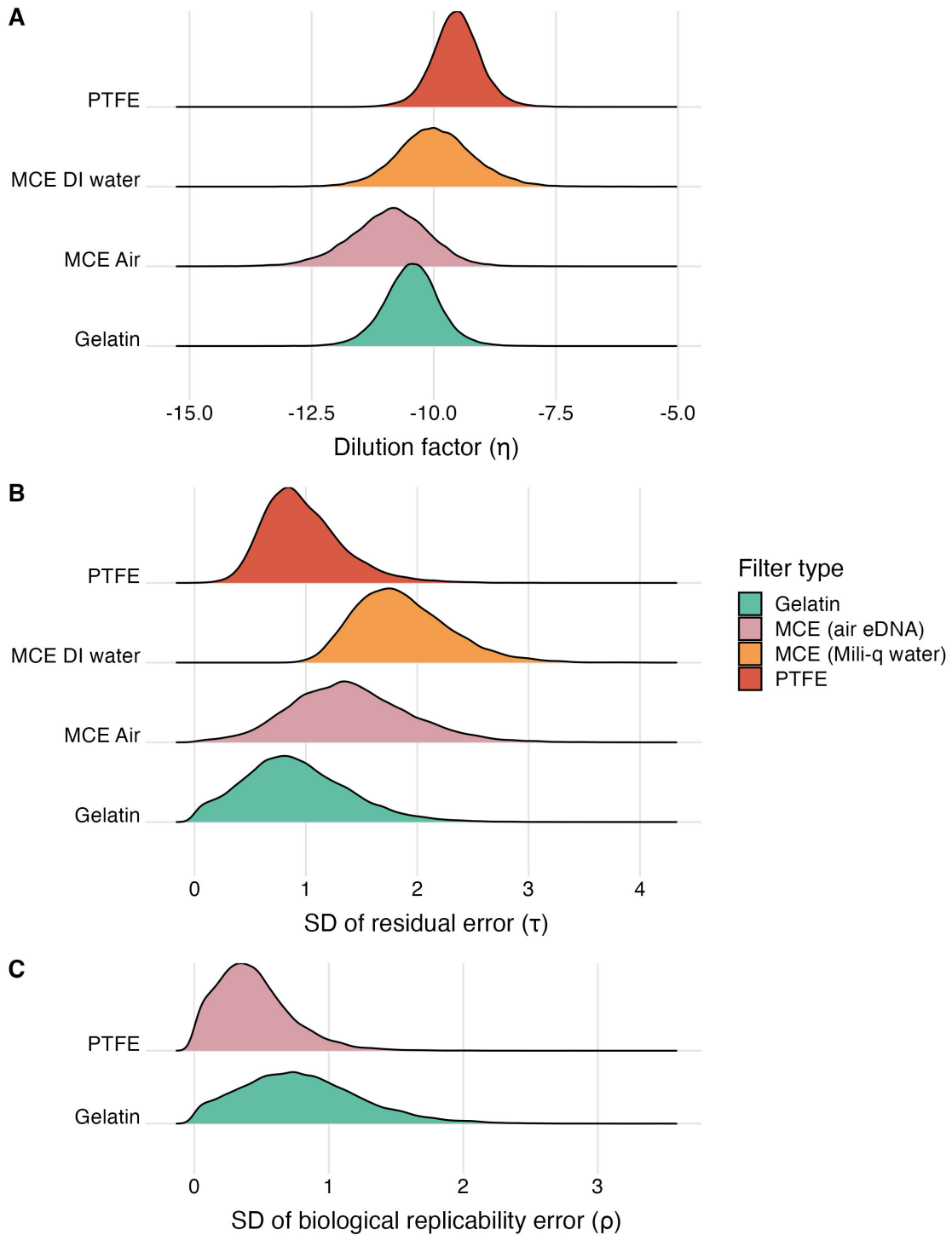


Figure 2: Density plots showing posterior distributions of: (A) water-to-air dilution factors (η), illustrating the magnitude of concentration reduction between aquatic and atmospheric matrices; (B) standard deviation (SD) of the residual error values (τ), representing the congruence (lower = better) between estimated eDNA concentrations between air and water; and (C) standard deviation (SD) of the biological replicability error (ρ), quantifying measurement consistency (lower = better) between technical replicates of two air filters (PTFE and gelatin filters). Each parameter is estimated for each of four different air eDNA collection methods (differentiated by colors).

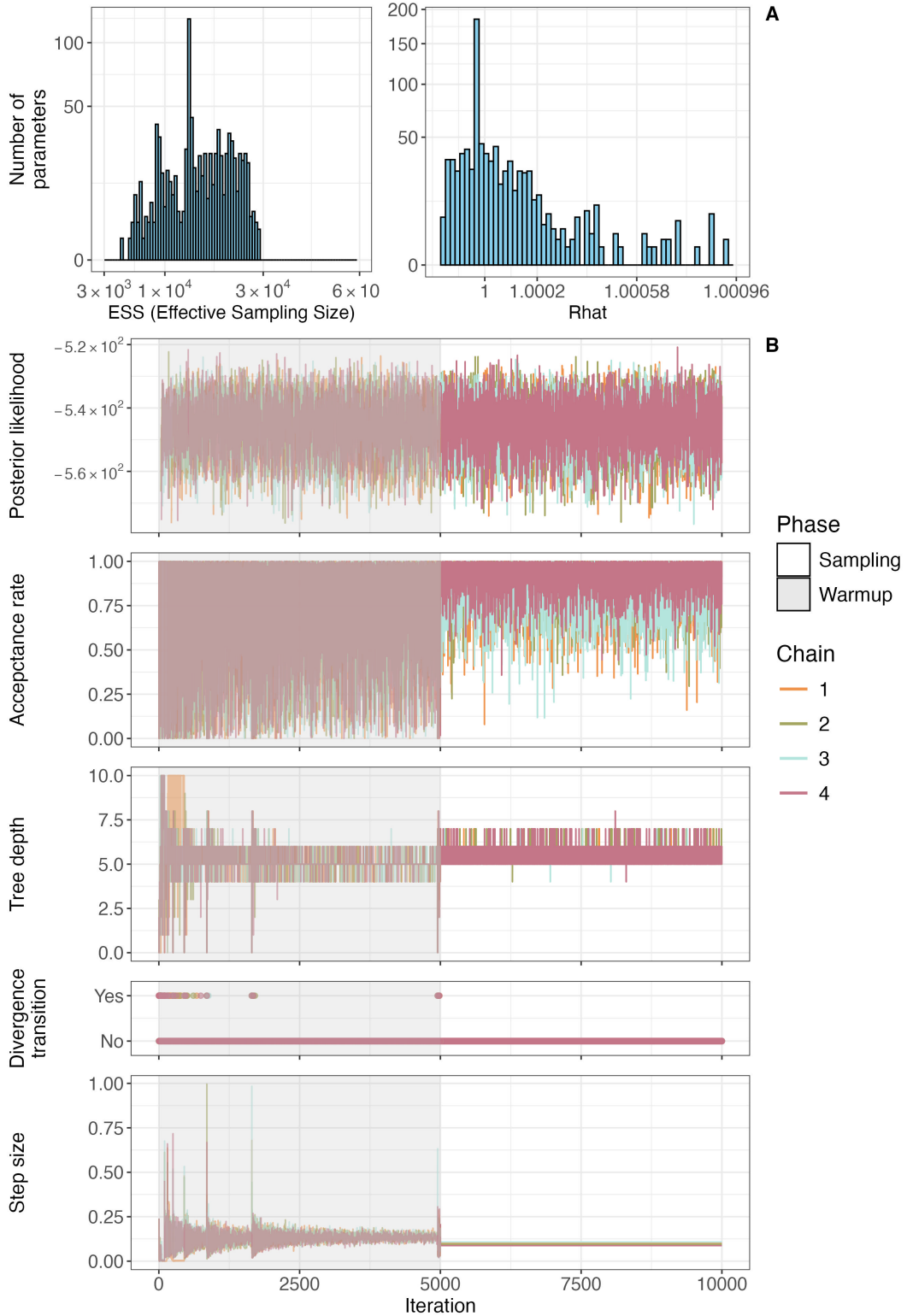


Figure 3: Bayesian model convergence diagnostics indicating (A) the distributions of effective sample size (ESS, left) and \hat{R} values (right) for all parameters and (B) convergence metrics across iterations, including posterior likelihood, acceptance rate, tree depth, divergence transitions, and step size for four MCMC chains. Warmup and sampling phases are distinguished by background shading.

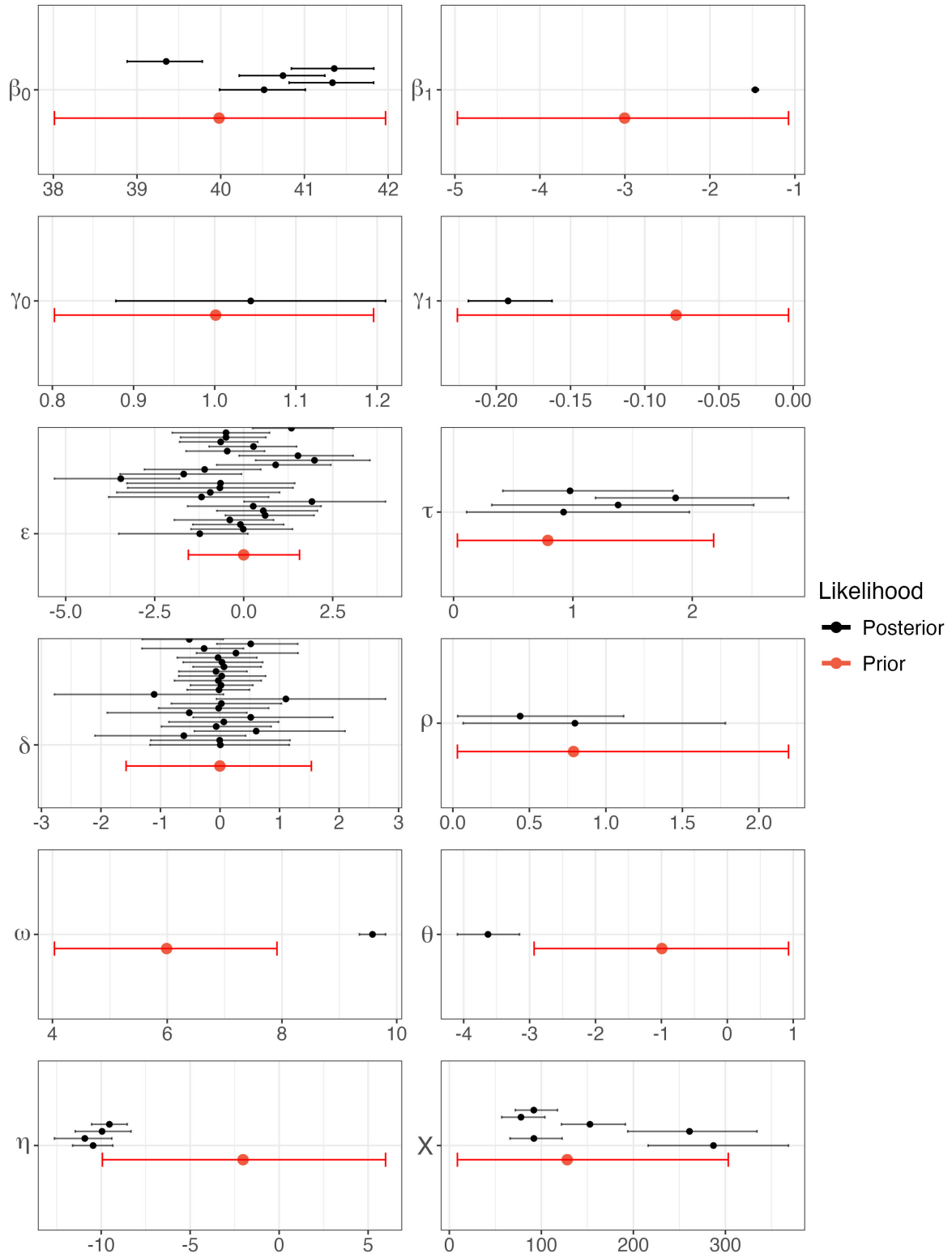


Figure 4: Prior sensitivity analysis for model parameters ($\beta_0, \beta_1, \gamma_0, \gamma_1, \varepsilon, \tau, \delta, \rho, \omega, \theta, \eta, X$). Black points and intervals represent posterior means and 95% confidence intervals respectively and red points and intervals show prior mean and 95% confidence intervals respectively.

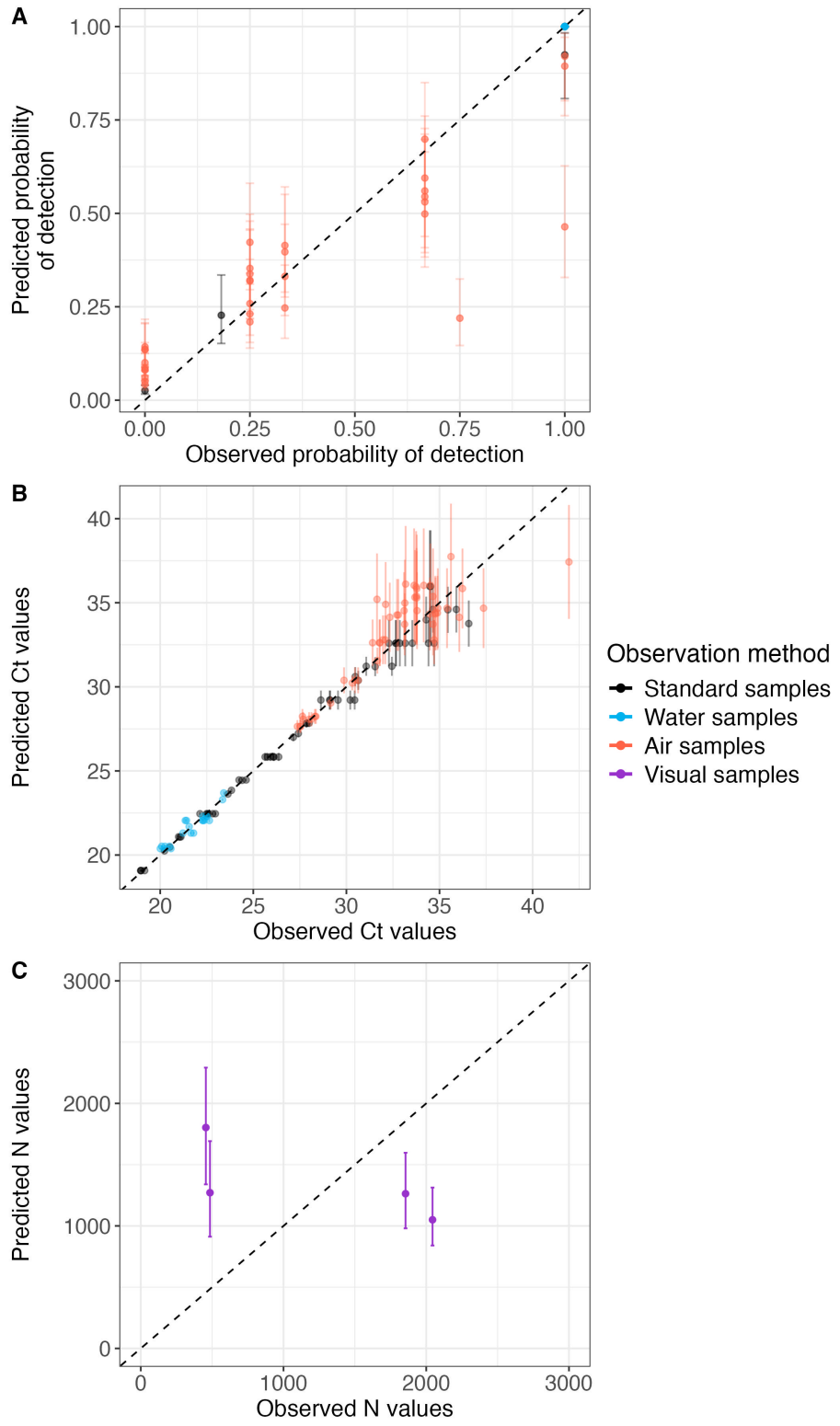


Figure 5: Posterior predictive checks comparing observed vs. model-predicted values for (A) detection probability of air and water samples alongside standard samples, (B) Ct values for air and water samples alongside standard, and (C) visual counts of fish (N).

Description	Prior
Data	
N number of fish counted	-
E elapsed days between counting	-
Z qPCR amplification (yes=1; no=0)	-
Y qPCR cycle threshold (C_t)	-
K known DNA concentration (qPCR standards)	-
V Reaction volume in μL	-
S Surface area of air collection method cm^2	-
State processes	
X unknown fish density in ($\text{fish} \cdot \text{day}^{-1}$)	$\mathcal{T}\mathcal{N}(100, 100; 0, +\infty)$
W unknown DNA concentration in water in (copies/L)	-
U unknown eDNA concentration in water samples (copies/ μL)	-
A unknown DNA concentration in air in (copies/day/ cm^2)	-
Q unknown eDNA concentration in air samples (copies/ μL)	-
Transformed parameters	
λ expected fish accumulated over E days	-
ψ probability of positive qPCR amplification	-
μ mean C_t values of qPCR	-
σ standard deviation of qPCR C_t values	-
Fixed parameters	
ϕ overdispersion parameter of Negative Binomial	- ($\phi = 20$)
Parameters	
ω conversion parameter between fish density and DNA concentration	$\mathcal{N}(6, 1)$
η dilution factor of DNA concentration from water to air	$\mathcal{N}(-2, 4)$
ε time (t) specific error term (residual)	$\mathcal{N}(0, \tau)$
τ standard deviation of residuals	$\mathcal{T}\mathcal{N}(0, 1; 0, +\infty)$
δ biological replicate error term (residual)	$\mathcal{N}(0, \rho)$
ρ standard deviation of biological replicate error	$\mathcal{T}\mathcal{N}(0, 1; 0, +\infty)$
θ intercept of the qPCR probability of detection (ψ) relationship and eDNA concentration (K , W , and A)	$\mathcal{N}(-1, 1)$
β_0 intercept of the linear relation between the mean C_t values (μ) and eDNA concentration (K , W , and A)	$\mathcal{N}(40, 1)$
β_1 slope of the linear relation between the mean C_t values (μ) and eDNA concentration (K , W , and A)	$\mathcal{N}(-3, 1)$
γ_0 intercept of the linear relation between the standard deviation of C_t values (σ) and eDNA concentration (K , W , and A)	$\mathcal{N}(1, 0.1)$
γ_1 intercept of the linear relation between the standard deviation of C_t values (σ) and eDNA concentration (K , W , and A)	$\mathcal{N}(0, 0.1)$
Index	
t time (days)	-
j filter type	-
b biological sample replicate	-
p qPCR plate	-
k qPCR standard sample	-
r qPCR technical replicate	-

Table 1: Data, state processes, parameters, transformed parameters, and subscripts employed in the joint Bayesian model and their prior distributions